

# Spectroscopic study of cataphoresis in He-Cd mixtures: Cd source-anode region

J. Mizeraczyk

*Institute of Fluid Flow Machinery, Polish Academy of Sciences, 80-952 Gdańsk, Poland*

C. Carlsson and S. Hård

*Chalmers University of Technology, Department of Applied Electron Physics, 41296 Göteborg, Sweden*

(Received 10 July 1991; accepted for publication 31 March 1992)

The results of measurements of the axial distributions of the Cd 479.9 nm, Cd<sup>+</sup> 441.6 nm, and He 447.2 nm line intensities as a result of cataphoresis in a He-Cd capillary positive column (3 mm diam) between the Cd source, placed at the cathode side, and the anode are presented. The measurements were carried out using optical scanning along the positive column. The measuring procedure also allowed the Cd atom density distributions along the positive column to be determined. It is found that the He-Cd positive column divides into three regions: the seemingly uniform, blue-colored cadmiumlike discharge region, the whitish transition region, and the orange heliumlike discharge region. The Cd atom density decreases linearly from the Cd source towards the anode in the cadmiumlike discharge region of the positive column. In the transition region the Cd atom density decreases quasiexponentially, extending its tail into the heliumlike discharge region. The very tail of the Cd atom density distribution found in the heliumlike region is perhaps not real. Instead it could be due to misinterpretation of scattered background light for fluorescence light. This ambiguity makes it impossible to draw any definite conclusion about the ability of cataphoresis to confine the Cd vapor at the cathode side of the positive column. It is found that particularly the linear but also the quasiexponential decrease of the Cd atom density, occurring in the He-Cd positive column, are in good agreement with Druyvesteyn's theory [*Physica* 2, 255 (1935)]. The slope of the Cd atom density distribution curve in its linear part was found to be proportional to the product of the discharge current and He pressure, whereas in its quasiexponential part it first increases and then saturates with increasing discharge current and He pressure. The results obtained can be used for estimating the so-called cataphoretic confinement section length for the positive column and hollow-cathode discharge He-Cd<sup>+</sup> lasers, as well as for other ion He-metal-vapor lasers. The features of cataphoresis in the He-Cd positive column found also seem to be characteristic of cataphoresis in other binary gas mixtures.

## I. INTRODUCTION

It is well known that if a dc glow discharge is operated in a binary mixture of gases consisting of a main gas and an admixture gas of a lower ionization potential, the preferentially ionized admixture gas will be transferred to the region near the cathode. This phenomenon, which also can occur in multicomponent gas mixtures, is termed cataphoresis. Cataphoresis, or the selective transport of the preferentially ionized constituent (or constituents in multicomponent mixtures) of a gas mixture towards the cathode, is used for gas purification, isotopic enhancement and, recently, in ion He-metal-vapor lasers. The theoretical and experimental studies in this area have been summarized in the comprehensive surveys by Laška<sup>1</sup> and Chanin.<sup>2</sup>

Cataphoresis has been employed for two purposes in ion He-metal-vapor lasers.<sup>3</sup> First, in the so-called positive column (PC) ion He-metal-vapor lasers cataphoretic transport of the metal-vapor particles from the metal source towards the cathode has been used to establish a uniform distribution of the optically active metal-vapor ions along the PC.<sup>4-6</sup> Second, in both PC and so-called hollow-cathode-discharge (HCD) lasers cataphoretic action between the metal source and the anode has been used

for confinement of the metal vapor in the tube section where the discharge excitation of the laser states occurs.<sup>7,8</sup>

The confinement of metal vapor to the excitation section of the discharge tube and prevention of metal-vapor diffusion out of it are current technology problems of both PC (325.0 and 441.6 nm) and HCD (441.6, 533.7, 537.8, 635.5, and 636.0 nm, resulting in the so-called white-light laser beam) He-Cd<sup>+</sup> lasers. Two ways of realizing confinement are shown in Fig. 1. In both schemes the Cd diffusion preventing action of cataphoresis occurs in the so-called cataphoretic confinement sections in which the main or auxiliary glow discharges produce positive columns whose axial electric fields make the Cd<sup>+</sup> ions drift toward the excitation section, located at the cathode-side region of the glow discharges. This Cd<sup>+</sup> ion drift towards the excitation section counteracts the Cd particles' (atoms and ions) diffusion occurring in the opposite direction, away from the excitation section. The confinement efficiency of the Cd particles to the excitation section is given by the difference between the drift flow of the Cd<sup>+</sup> ions and the diffusion flow of the Cd particles. Perfect confinement of Cd particles to the excitation section of the discharge tube is desirable in He-Cd<sup>+</sup> lasers.

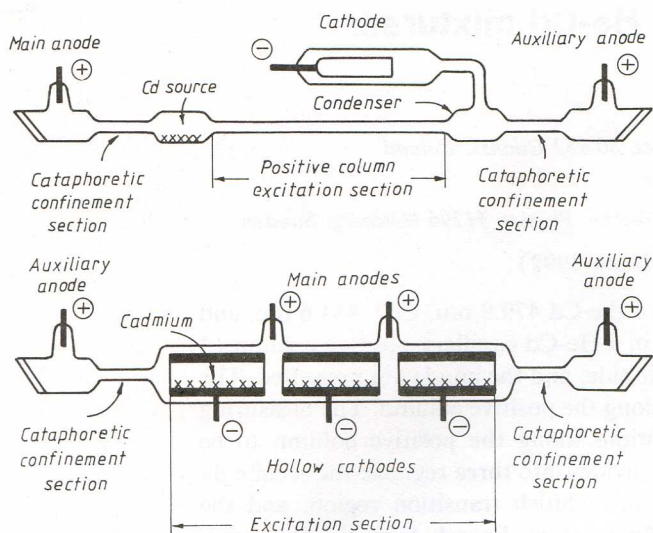


FIG. 1. Drawings of the He-Cd PC (upper scheme) and HCD laser tubes showing the cataphoretic confinement sections preventing diffusion of Cd particles out of the excitation regions.

However, there exists a controversy regarding the cataphoretic confinement efficiency of Cd particles to the discharge tube excitation section or, more generally, to the cathode-side region of a glow discharge, when using cataphoretic confinement sections. According to the commonly accepted theory developed by Sosnowski<sup>6</sup> for cataphoresis in He-Cd laser mixtures, the confinement of Cd particles to the cathode region is never perfect. However, in this as well as in many similar experiments Hernquist<sup>8</sup> and ourselves were not able to see any traces of cadmium having diffused out of the cathode region of the discharge after 1000 h of operation. Other literature data on cataphoresis, including the surveys of Laška<sup>1</sup> and Chanin,<sup>2</sup> do not help in settling the controversy.

The above ambiguity on the cataphoretic confinement efficiency stimulated us to make this study on cataphoresis action in a He-Cd capillary positive column between a Cd source, placed near the cathode, and the anode. Aside from a better understanding of cataphoresis, the study might help improve the design and performance of He-Cd<sup>+</sup> lasers, as well as other ion He-metal-vapor lasers.

## II. EXPERIMENTAL PROCEDURE

A schematic of the He-Cd discharge tube used in this study is shown in Fig. 2. The tube consisted of three parts: the cathode region, the capillary PC section, and the anode region. The cathode region consisted of a hollow cathode made of Kovar, and a Cd source, being a Kovar glass tube in which pieces of cadmium were placed. The capillary PC section, in which the cataphoresis was to be investigated, was made of a 45-mm-long Pyrex glass tube with an inner diameter of 3 mm. A tungsten anode rod, a glass tube outlet to the vacuum system, and a control end-light window were situated in the anode region.

Separate ovens were provided for the cathode, the Cd source, the capillary section, and the anode so that their temperatures could be controlled independently. Regard-

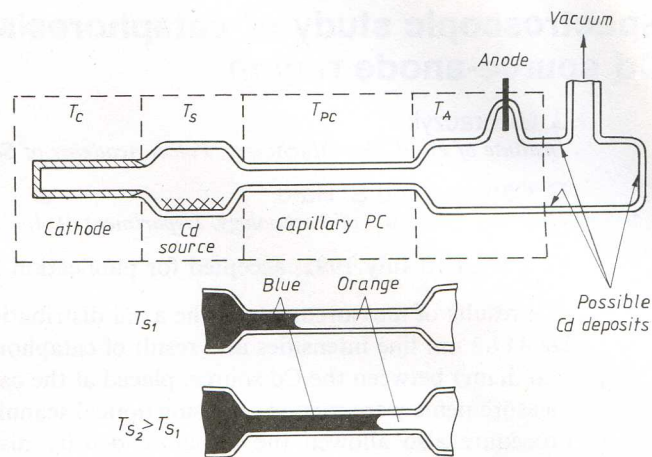


FIG. 2. The experimental tube used for the study of cataphoresis between the Cd source and the anode in the He-Cd PC. The appearance of the He-Cd PC for two different temperatures of the Cd source ( $T_{S1}$ ,  $T_{S2}$ ) are also shown.  $T_C$ ,  $T_S$ ,  $T_{PC}$ , and  $T_A$  are the temperature of the cathode, Cd source, capillary PC, and anode, respectively.

less of the discharge conditions, the temperatures of the cathode  $T_C$ , the capillary section  $T_{PC}$ , and the anode  $T_A$  were always kept at 663 K, which was well above the temperature of the Cd source  $T_S$ . This prevented condensation of Cd atoms on the inner walls of the cathode, the capillary section, and the anode. By avoiding Cd deposition on the capillary PC inner walls, subsequent desorption of Cd particles due to the interaction of plasma ions and excited particles with the walls of the discharge tube was eliminated. Desorption, being an uncontrolled source of an admixture gas, apparently occurred in previous investigations (Krysmanski<sup>9</sup> in He-Kr, Tombers, Gaur, and Chanin<sup>10</sup> in He-N<sub>2</sub>, Tombers and Chanin<sup>11</sup> in Ne-Hg and Ne-Xe-Hg, and Hackam<sup>12</sup> in Ne-Ar mixtures). In our case the only places where Cd atoms could deposit were at the Cd source, when cooled, or at the cold parts of the tubing outside the anode oven (see Fig. 2). Keeping the temperatures  $T_C$ ,  $T_{PC}$ , and  $T_A$  constant was necessary because of the temperature dependence of cataphoresis and because it kept the main gas density in the capillary section constant, regardless of the discharge current variations.<sup>12-20</sup> The discharge tube was connected to a large-volume gas reservoir, so that the He atom density in the capillary section at a temperature of 663 K was equal to half the initial He atom density at room temperature. Consequently, the He pressure values given in this paper are half the initial He pressures. A narrow slot was made in the oven surrounding the capillary section to allow observations of the PC.

Prior to placing the Cd pieces into the Cd source, the Cd pellets were carefully distilled in vacuum. The discharge tube with the Cd pieces in the Cd sources was cleaned by pumping, baking (all parts of the tube except the Cd source up to 693 K), and running the discharge during several days.

The experimental procedure was as follows. First, a discharge was started at a constant discharge current  $I$ , He pressure  $p$ , and temperatures  $T_C$ ,  $T_{PC}$ , and  $T_A$  fixed at 663

K. Since at this point the Cd source was not heated ( $T_S < 343$  K) and there was practically no Cd vapor in the discharge, the PC had a uniform, characteristic He orange color along all its length. Then, the Cd source temperature was raised and Cd vapor appeared in the discharge. This resulted in a change of the color of the PC of the discharge. The capillary PC was sharply divided into two parts: one near the Cd source showed blue light characteristic of a Cd discharge, whereas the remaining part at the anode side showed pure He discharge orange-light emission (Fig. 2). The boundary between the two parts, whitish in color, was spherical. The length of the blue-colored part of the capillary PC could be varied by varying the Cd source temperature. The higher the Cd source temperature, the longer the blue-colored part of the capillary PC, as shown in Fig. 2.

Therefore, the naked-eye observations described above suggest the existence of three regions in the He-Cd capillary PC. The first region, near the Cd source, contains helium and a relatively high concentration of Cd vapor. The second region, at the anode side, contains helium with little or no Cd vapor at all. The whitish layer is a transition region between the two main regions.

Presence of Cd atoms in the capillary PC was detected by side monitoring the characteristic blue spectral line fluorescence of cadmium at 479.9 nm. As measured in a supplementary experiment (see the Appendix) the Cd 479.9 nm line intensity in the He-Cd PC is approximately proportional to the density of Cd atoms in the ground state if the Cd atom density in the PC is below  $15 \times 10^{12} \text{ cm}^{-3}$ . At higher Cd atom densities the Cd 479.9 nm line intensity saturates and the proportionality between the Cd 479.9 nm line intensity and the density of Cd atoms in the ground state ceases. However, having measured the intensity of the Cd 479.9 nm spectral line emitted by the PC, the calibration curves obtained in the supplementary experiment could be used to determine the density of Cd atoms in the ground state in the He-Cd PC up to  $100 \times 10^{12} \text{ cm}^{-3}$ .

The sidelight emission at 479.9 nm was measured along the center of the capillary PC through a 2-mm-wide longitudinal slot in the capillary PC oven either by directly placing an optical fiber close to the capillary or by imaging the emission from the center of the capillary PC onto an optical fiber. The fiber core diameter was 0.2 mm in the former case and 0.6 mm in the latter. The spatial resolution along the tube axis of the two measuring setups is estimated at about 1.5 mm. The light gathered by either fiber was transmitted to a monochromator with an attached photomultiplier having an amplifier and a voltmeter at its output. Scanning along the capillary PC was done in 0.5 mm steps using a micrometer screw. While very similar results were obtained with either measuring setup, most results were collected with the directly measuring setup and these are presented in this paper.

Aside from measuring the Cd 479.9 nm line intensity, the intensities of the Cd<sup>+</sup> 441.6 nm laser line and the He 447.2 nm line were also regularly measured as a function of distance along the capillary PC. Often the intensity distri-

butions of several other He, Cd, and Cd<sup>+</sup> lines were also measured.

Although the capillary PC was kept at a temperature well above the Cd vapor condensation temperature, deposits of an unknown origin gradually formed on the inner wall of the capillary during the course of the experiment. The deposits irregularly altered the light transmittivity through the capillary wall from point to point along the capillary. As a result, the measured sidelight intensity distributions along the capillary PC were distorted. We tried to correct the measured intensity with a simple data calibration procedure previously used by Sosnowski.<sup>6</sup> In brief, Sosnowski's procedure is as follows: First, the intensity of a He reference line (the He 492.1 nm line in the Sosnowski experiment, the much stronger He 447.2 nm line our case) versus capillary PC distance was recorded with no cadmium in the discharge. Then the intensities of the He and Cd lines obtained in the regular measurement were divided at each measuring point by the intensity of the He reference line measured at the same point. Assuming that the quotient of the light transmittivities of the capillary wall for the He and Cd lines is constant along the capillary, the data calibration process should result in the true spectral line intensity distributions. The intensity of the He reference line was always measured before and after each measuring series comprising the Cd 479.9 nm, Cd<sup>+</sup> 441.6 nm, and He 447.2 nm lines. We found that the He reference line intensity did not alter significantly during a measuring series.

The measurements were carried out for various He pressures and discharge currents ranging from 4 to 25 mbar, and from 15 to 155 mA, respectively. The Cd density in the Cd source, determined from the temperature of the Cd source, ranged up to  $500 \times 10^{12} \text{ cm}^{-3}$ , where the temperature dependence of Cd-saturated vapor pressure was taken from Roth.<sup>21</sup>

A difference should be noted between this experiment and most other experiments on cataphoresis in gas mixtures. In the latter cases (summarized by Laška<sup>1</sup> and Chanin<sup>2</sup>), the discharge tubes were initially uniformly filled with a mixture of gases, including metal-vapor constituents, and cataphoresis was investigated after initiating the discharge. As a result, a spatial redistribution of the mixture constituents occurred, with the preferentially ionized admixture gas gathering near the cathode. However, due to tube geometry and discharge condition dependence, the admixture gas density at the cathode side of the discharge tube could not be well controlled. This might have been one of the reasons for difficulties in interpreting the discharge current dependence of cataphoresis met by other authors (Tombers and co-workers<sup>10</sup> in He-N<sub>2</sub>, Tombers and Chanin<sup>11</sup> in Ne-Hg and Ne-Xe-Hg, Hackam<sup>12,20</sup> in Ne-Ar and He-Ar, Schmeltkopf<sup>14</sup> in He-Ne, Gaur and Chanin<sup>18,22</sup> in He-Ne and He-Ar, and Hackam and Vincent<sup>23</sup> in He-Ar mixtures). In contrast, in this experiment (as well as in the experiments of Sosnowski<sup>6</sup> and Muller and Tubbs<sup>24</sup> on the He-Cd and Ne-Hg mixtures, respectively) the final Cd atom density in the cathode region of the discharge tube was not the result of cataphoresis but

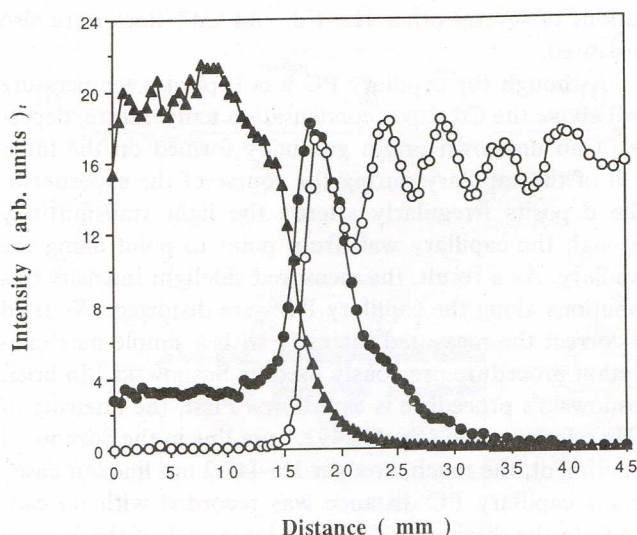


FIG. 3. Axial distributions of the intensities of the Cd 479.9 nm ( $\blacktriangle$ ),  $\text{Cd}^+$  441.6 nm ( $\bullet$ ), and He 447.2 nm ( $\circ$ ) lines between the Cd source (at 0 mm) and the anode in the He-Cd PC. Discharge parameters:  $p=4$  mbar,  $I=85$  mA,  $T_S=550.5$  K.

was determined by the controlled Cd source temperature. The independent control of admixture gas density at the cathode side of the PC helped in interpreting the measurements.

### III. EXPERIMENTAL RESULTS

The intensities of the spectral lines presented below are given in arbitrary units. While in some cases the measured values for different spectral lines were multiplied by different factors because of presentation requirements, the relative values for a specific line are preserved regardless of the measuring conditions. The original ratio between the strongest intensities of the Cd 479.9 nm,  $\text{Cd}^+$  441.6 nm, and He 447.2 nm lines was approximately 4:1:3.

A typical result of an axial distribution measurement of the sidelight intensities of the Cd 479.9 nm,  $\text{Cd}^+$  441.6 nm, and He 447.2 nm lines along the He-Cd PC is shown in Fig. 3. It confirms the naked-eye observation that the He-Cd PC between the Cd source and the anode is divided into three regions. In the region near the Cd source, extending to almost  $\frac{1}{3}$  of the PC for the conditions presented in Fig. 3, the emission of atomic Cd spectral lines dominates, the intensities of ionic  $\text{Cd}^+$  lines are weak, and the intensities of atomic He lines are negligible. Visually this region appears blue. A reverse behavior of the atomic He and Cd line intensities is observed at the anode side of the He-Cd PC, which visually appears orange. The intensities of ionic  $\text{Cd}^+$  lines are weak or negligible in the latter region. Between the two regions a transition region exists (the whitish region mentioned above) where the intensities of atomic Cd lines decrease and the intensities of atomic He lines increase towards the anode. The  $\text{Cd}^+$  441.6 nm line intensity reaches a maximum in this region.

The strong emission of the Cd atomic lines and the low intensities of the He lines and the  $\text{Cd}^+$  441.6 nm line,

observed in the region near the Cd source, are brought about by a relatively high density of Cd atoms in this part of the PC. As a result, the electron density decreases so that the excitation of the upper-lying lines is low (see, e.g., Ref. 25). The steep decrease and increase of the Cd 479.9 nm line intensity and He 447.2 nm line intensity, respectively, occurring in the transition region, are due to a rapid decrease of the Cd atom density and increase of the electron energy accompanying it. The decrease of the densities of both Cd atoms and  $\text{Cd}^+$  ions and the increase of the electron energy in the transition region results in the maximum of the  $\text{Cd}^+$  441.6 nm line excitation.<sup>26,27</sup> The disappearance of the atomic Cd and ionic  $\text{Cd}^+$  line fluorescence as well as the high intensity of the He 447.2 nm line, equal in magnitude to that of a pure He PC, in the near-anode part of the PC suggest that this region contains very little or no cadmium.

Two facts need special comment. First, the intensity of the Cd 479.9 nm line, as well as the other Cd lines, increases rapidly in the transition region in going toward the Cd source, reaches a maximum, and then even decreases in the region adjacent to the Cd source (Fig. 3). However, that does not necessarily mean that the Cd atom density also reaches its maximum and then decreases. The results of the supplementary experiment (see Appendix) suggest that saturation of the atomic Cd line intensities can be expected if the Cd atom density is high in the region near the Cd source. Similar intensity saturation of the atomic lines of the admixture constituents near the cathode was also observed by Hackam<sup>12,20</sup> in Ne-Ar and He-Ar, Hackam and Vincent<sup>23</sup> in He-Ar, Malyshev and Pavlov<sup>28</sup> in Ne-Hg, Morgenroth<sup>29</sup> in Ar-Hg, and Springer and Barnes<sup>30</sup> in Ar-Cd and Ne-Cd mixtures. Second, the intensity of the He 447.2 nm line, as well as the other He lines, showed regular variations, so-called standing striations,<sup>31</sup> along the PC near the anode (Fig. 3). It is highly probable that the large ionization rate gradient in the transition region is the cause of the standing striations observed in the PC region near the anode.<sup>32</sup>

In previous investigations of cataphoresis the so-called quality of cataphoresis was defined as the distance from the anode to a point of the PC at which a marked change in the atomic admixture line intensity occurs.<sup>12,14</sup> In the case of He-Cd mixtures it is convenient to use the position of the  $\text{Cd}^+$  441.6 nm line intensity maximum along the PC as an indicator of the location of the demarcation point (or transition region) between the cadmiumlike and heliumlike discharge regions of the PC, or, in other words, as a measure of the quality of cataphoresis. The positional shifts  $\Delta x$  of the  $\text{Cd}^+$  441.6 nm line intensity maximum along the PC due to variations of the Cd atom density in the Cd source  $\Delta N$ , the discharge current  $\Delta I$ , and the He pressure  $\Delta p$  depend upon whether the Cd atom density in the Cd source  $N$  is lower or higher than that above which the Cd 479.9 nm line intensity saturates in the PC (Figs. 4–6). In both the present and the supplementary experiments (see Appendix) we found that the intensities of the atomic Cd lines in the He-Cd PC saturate if the Cd atom density in the Cd source is in excess of  $100 \times 10^{12} \text{ cm}^{-3}$ , termed  $N_S$ .

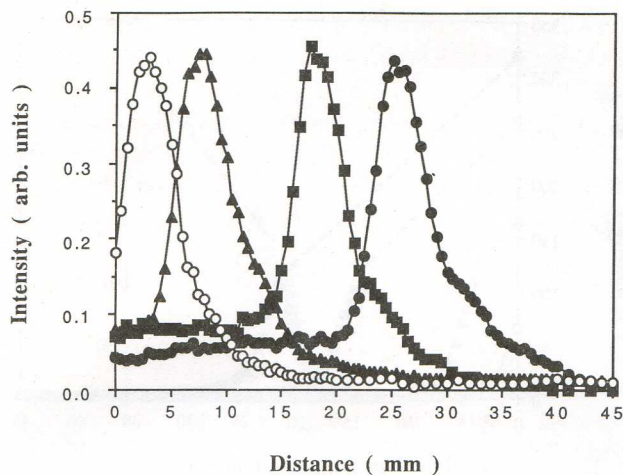


FIG. 4. Axial distributions of the  $\text{Cd}^+$  441.6 nm line intensity between the Cd source (at 0 mm) and the anode in the He-Cd PC for various temperatures of the Cd source.  $\circ$ : 520 K;  $\blacktriangle$ : 540 K;  $\blacksquare$ : 550.5 K;  $\bullet$ : 555.5 K. Other parameters:  $p=4$  mbar,  $I=85$  mA.

In general,  $\Delta x/\Delta N$ ,  $\Delta x/\Delta I$ , and  $\Delta x/\Delta p$  are higher for  $N > N_S$ , the other parameters being comparable. The quantity  $\Delta x/\Delta I$  is lower for the higher-discharge currents and saturates at about 155 mA. A similar behavior of the demarcation point was observed for other mixtures (e.g., for the He-Ne mixtures by Schmeltekopf,<sup>14</sup> Gaur and Chanin,<sup>18</sup> and for the He-Ar mixture by Hackam,<sup>12</sup> Gaur and Chanin,<sup>22</sup> and Hackam and Vincent<sup>23</sup>). The quantity  $\Delta x/\Delta p$  is lower for the higher He pressures and saturates at about 25 mbar. This is consistent with the results of studies of cataphoresis in He-Ne and He-Ar mixtures carried out by Schmeltekopf<sup>14</sup> and Gaur and Chanin,<sup>22</sup> respectively.

Typical numerical examples of  $\Delta x$  in a He-Cd mixture are as follows: (a) at  $p=4$  mbar and  $I=85$  mA:  $\Delta x/\Delta N \approx 0.05 \times 10^{-13} \text{ cm}^4$  at  $N < N_S$ ,  $\Delta x/\Delta N \approx 0.1 \times 10^{-13} \text{ cm}^4$  at  $N > N_S$ ; (b) at  $p=4$  mbar, at  $N < N_S$ :  $\Delta x/\Delta I \approx 1$  mm/mA

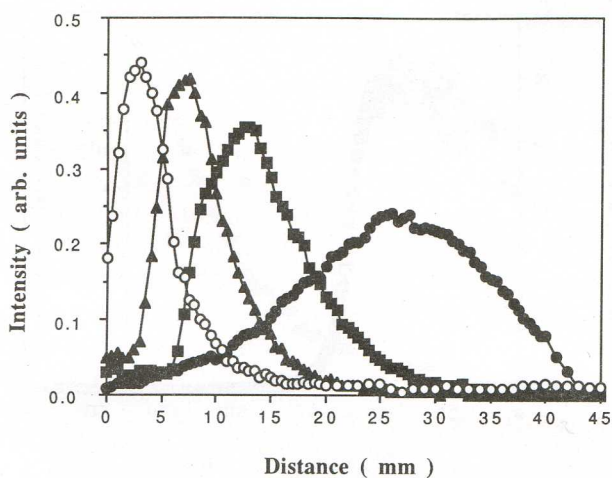


FIG. 5. Axial distributions of the  $\text{Cd}^+$  441.6 nm line intensity between the source (at 0 mm) and the anode in the He-Cd PC for various discharge currents.  $\circ$ : 85 mA;  $\blacktriangle$ : 50 mA;  $\blacksquare$ : 30 mA;  $\bullet$ : 15 mA. Other parameters:  $p=4$  mbar,  $T_S=520$  K.

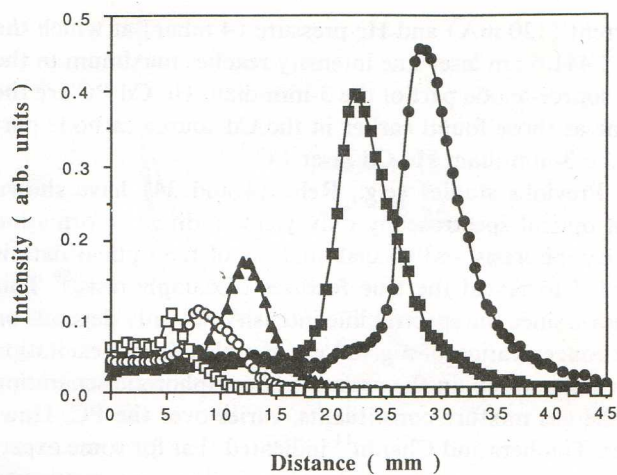


FIG. 6. Axial distributions of the  $\text{Cd}^+$  441.6 nm line intensity between the Cd source (at 0 mm) and the anode in the He-Cd PC for various He pressures.  $\square$ : 25.3 mbar;  $\circ$ : 16 mbar;  $\blacktriangle$ : 12 mbar;  $\blacksquare$ : 8 mbar;  $\bullet$ : 4 mbar. Other parameters:  $I=50$  mA,  $T_S=550.5$  K.

for  $I=(15-30)$  mA,  $\Delta x/\Delta I \approx (0.07 \pm 0.04)$  mm/mA for  $I=(50-85)$  mA; at  $p=4$  mbar, at  $N > N_S$ :  $\Delta x/\Delta I \approx 0.3$  mm/mA for  $I=(50-85)$  mA,  $\Delta x/\Delta I \approx 0.06$  mm/mA for  $I > 120$  mA; (c) at  $I=50$  mA, at  $N > N_S$ :  $\Delta x/\Delta p \approx (0.15 \pm 0.05)$  mm/mbar; at  $I=50$  mA, at  $N > N_S$ :  $\Delta x/\Delta p \approx 2.4$  mm/mbar for  $p=(4-8)$  mbar,  $\Delta x/\Delta p \approx 0.2$  mm/mbar for  $p=(16-25.3)$  mbar.

Besides the shift in  $\Delta x$ , the slope of the Cd 479.9 nm line intensity distribution curve also gives a measure of the efficiency of the cataphoresis. Our measurements showed that the slope of the axial distribution curve of the Cd 479.9 nm line intensity is inversely proportional to the width of the bell-shaped axial distribution of the  $\text{Cd}^+$  441.6 nm line intensity within the transition region. Therefore, the width of the  $\text{Cd}^+$  441.6 nm line intensity distribution curve can be used as a measure of the slope of the Cd 479.9 nm line intensity distribution curve. This close relation between the width and slope of the relevant distribution curves allows the following conclusions about the slope of the Cd 479.9 nm line intensity distribution curve in the transition region to be drawn from Figs. 4-6: (a) The slope is independent of the Cd atom density in the Cd source; (b) the slope primarily increases and then saturates with increasing discharge current and He pressure. Similar discharge current and main gas pressure dependencies for the slope of the axial distribution curve of either the intensity of the characteristic atomic line or the ion species of the admixture gas in the relatively fast decaying region of the distribution, termed the transition region in the present work, can also be observed in the previous investigations of cataphoresis in He-Ne (Ref. 14—He pressure dependence, Refs. 18 and 33), He-Kr,<sup>19</sup> He-Ar,<sup>20,22,23</sup> He-N<sub>2</sub>,<sup>10</sup> Ne-Hg (Ne pressure dependence) and Ne-Xe-Hg (discharge current dependence),<sup>11</sup> Ne-Ar (discharge current dependence valid for higher Ne pressures only),<sup>12,33</sup> and Kr-Xe mixtures (discharge current dependence at higher Kr pressures).<sup>33</sup>

It is also worth noticing that the optimum discharge

current (120 mA) and He pressure (4 mbar) at which the  $\text{Cd}^+$  441.6 nm laser line intensity reaches maximum in the Cd source-anode part of the 3-mm-diam He-Cd PC are the same as those found earlier in the Cd source-cathode part of the 3-mm-diam He-Cd laser PC.<sup>3</sup>

Previous studies (e.g., Refs. 14 and 34) have shown that optical spectroscopy only yields indirect information on cataphoresis and special analysis of the optical data is needed to reveal the true features of cataphoresis.<sup>29</sup> This follows since the spectral line intensity not only depends on the concentration of a given gas but also on the excitation efficiency which, in the presence of cataphoretic separation of the gas mixture constituents, varies over the PC. However, Tombers and Chanin<sup>11</sup> indicated that for some experimental conditions the results of optical measurements can be as informative as those obtained by mass spectroscopy. The usefulness of optical data for quantitative analysis of cataphoresis in a He-Cd mixture is shown below.

Transformation of the Cd 479.9 nm line intensity distributions into Cd density distributions was done using the calibration curve of the Appendix, which gives the relation between the Cd 479.9 nm line intensity and the Cd atom density in the He-Cd PC. However, in the principal experiment the Cd 479.9 nm line intensity distributions along the He-Cd PC were measured in units different from those of the calibration curve. So, before the calibration curve could be used for the transformation, its ordinate axis had to be scaled so that the Cd 479.9 nm line intensities at the positions corresponding to the maximum of the  $\text{Cd}^+$  441.6 nm line intensity and ceasing of the He 447.2 nm line intensity were equal to the Cd 479.9 nm line intensities corresponding to the Cd atom densities of  $15 \times 10^{12} \text{ cm}^{-3}$  and  $100 \times 10^{12} \text{ cm}^{-3}$ , respectively, on the calibration curve. It is widely accepted (see, e.g., Refs. 27, 35–38, and the Appendix) that the  $\text{Cd}^+$  441.6 nm line intensity exhibits its maximum and the He 447.2 nm line intensity ceases at these particular Cd densities, respectively, in a 3-mm-diam He-Cd PC. Unfortunately, the saturated parts of the Cd 479.9 nm line intensity distributions could not be transformed into Cd atom density distributions in that way. The only point on the saturated part of the Cd 479.9 nm line intensity distribution curve that could be transformed reasonably reliably into Cd atom density is the very beginning of the PC, adjacent to the Cd source. The Cd atom density at the very beginning of the PC is assumed to be equal to the Cd atom density in the Cd source, which, in turn, can be calculated from the saturated vapor density versus Cd source temperature dependence.<sup>21</sup> As a result, for a series of Cd source temperatures, the Cd atom density distributions along the He-Cd PC could only be obtained in the form shown in Fig. 7, i.e., with the regions corresponding to the saturated parts of the Cd 479.9 nm line intensity distributions unknown (dashed lines) except at the point  $x=0$  mm.

However, it is characteristic of the Cd 479.9 nm line intensity distributions obtained for various Cd source temperatures, other parameters kept constant, that by parallel shifting the intensity distributions in the abscissa direction they can be made to overlap within experimental error

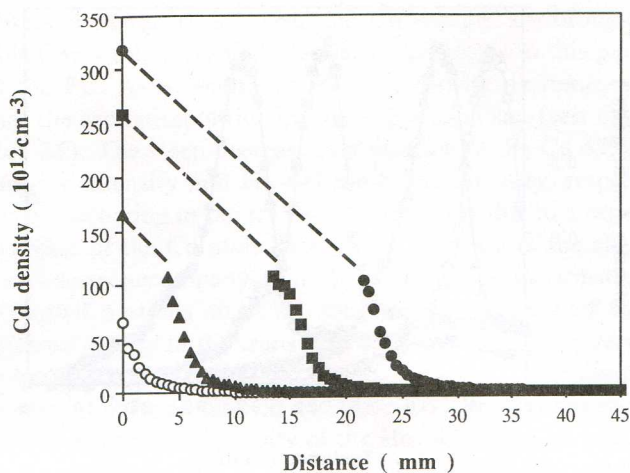


FIG. 7. Partial axial Cd atom density distributions between the Cd source (at 0 mm) and the anode in the He-Cd PC for various temperatures of the Cd source.  $\circ$ : 520 K;  $\blacktriangle$ : 540 K;  $\blacksquare$ : 550.5 K;  $\bullet$ : 555.5 K. Other parameters:  $p=4$  mbar,  $I=85$  mA.

forming a single so-called complete distribution, which is independent of the Cd source temperature (Fig. 8). Each of the Cd source temperature-dependent distributions of the Cd 479.9 nm line intensity is part of the corresponding complete distribution, and so each may be termed a partial distribution. The higher the Cd source temperature, the larger part of the complete distribution is the partial distribution.

Therefore, the regions of the Cd atom density distributions corresponding to the saturated parts of the Cd 479.9 nm line intensity distributions (Fig. 7) could be revealed by shifting the partial distributions in the abscissa direction thus forming the complete Cd atom density distribution (Fig. 9). The distribution thus obtained should show the shape of the true Cd atom density axial distribution between the Cd source and the anode in the He-Cd

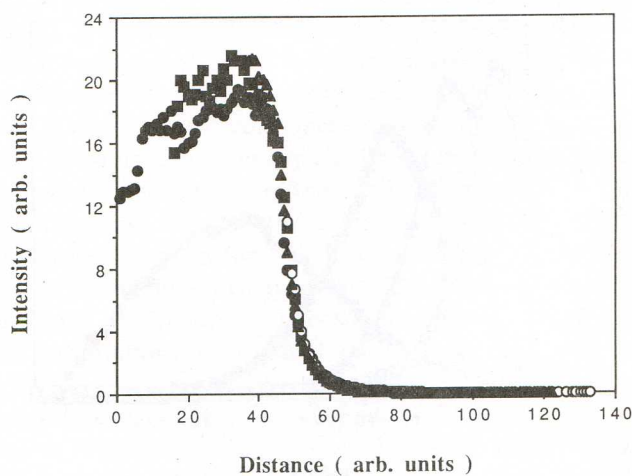


FIG. 8. Axial distributions of the Cd 479.9 nm line intensity obtained by shifting the measured distributions in the  $x$  direction until they overlap. Temperatures of the Cd source are  $\circ$ : 520 K;  $\blacktriangle$ : 540 K;  $\blacksquare$ : 550.5 K;  $\bullet$ : 555.5 K. Other parameters:  $p=4$  mbar,  $I=85$  mA.

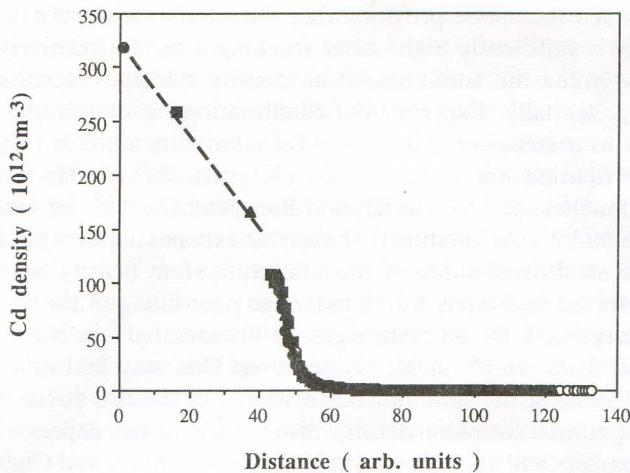


FIG. 9. Complete axial Cd atom density distribution between the Cd source (at 0 mm) and the anode in the He-Cd PC obtained after overlapping the distributions presented in Fig. 7.

PC. In general, the Cd atom density distribution consists of two parts. In the first part, near the Cd source, the Cd atom density decreases linearly with distance from the Cd source. In the second part, which extends over the transition and into the heliumlike discharge regions, the Cd atom density decreases more rapidly, similar to the decrease of the Cd 479.9 nm line intensity (Fig. 10), i.e., it first decreases exponentially and then slower and nonexponentially.

Using similar procedures as described above the discharge current and He pressure dependencies of the axial distributions of the Cd atom density in the He-Cd PC could be revealed. Figure 11 shows Cd atom density distributions at a relatively low Cd source temperature, for which only the second, quasiexponential part of the distributions exists. The slopes of the Cd atom density distribution curves, presented in Fig. 11, increase rapidly as the

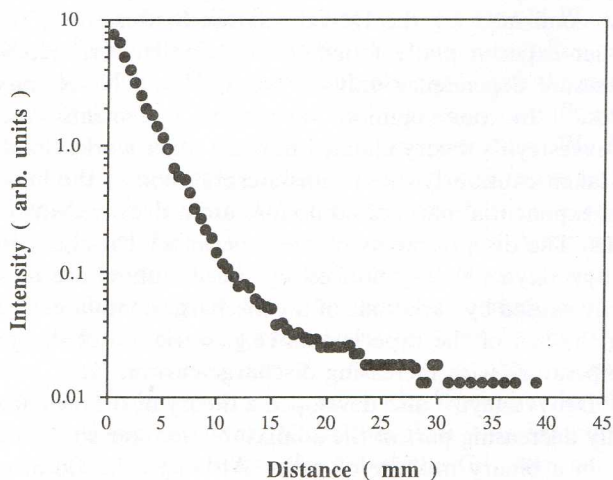


FIG. 10. An example of a measured axial distribution of the Cd 479.9 nm line intensity between the Cd source (at 0 mm) and the anode in the He-Cd PC shown in a log-linear scale. Discharge parameters:  $p=4$  mbar,  $I=85$  mA,  $T_S=520$  K.

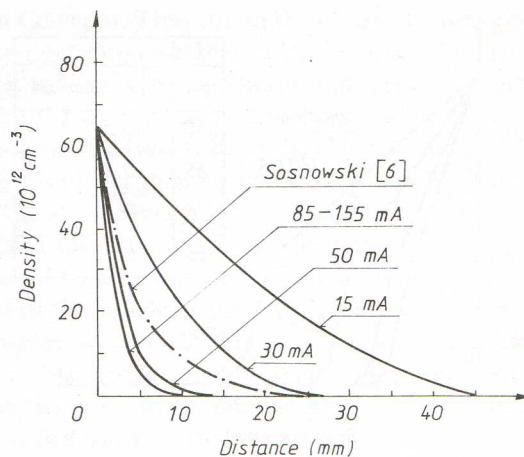


FIG. 11. Axial Cd atom density distributions between the Cd source (at 0 mm) and the anode in the He-Cd PC at a relatively low Cd source temperature (520 K) for various discharge currents, at  $p=4$  mbar. The dotted-dashed curve is based on Sosnowski's experiment (Ref. 6) (the tube diameter is 4 mm,  $p=3.6$  mbar,  $I=60$  mA,  $T_S=520$  K).

discharge current increases from 15 to 50 mA. Further increase of the discharge current does not change the slopes of the distribution curves significantly; in the range 85–155 mA the Cd atom density distributions are the same within experimental error. At a discharge current of 15 mA the Cd atom density distribution occupies all the He-Cd PC, whereas at higher discharge currents the bulk of the distribution is limited to the PC region adjacent to the Cd source. A relatively high Cd atom density at the anode side of the PC at 15 mA suggests that there might be a possible flow of Cd atoms through the PC and, thus, that there is Cd atom leakage. On the other hand, the confinement of the Cd atom density distributions to the neighborhood of the Cd source at discharge currents higher than 50 mA makes Cd atom flow and leakage less probable in that case. For comparison with our results, the Cd atom density distribution calculated from the data taken from the experiment of Sosnowski<sup>6</sup> is also presented (the dotted-dashed line) in Fig. 11. Taking the difference in the conditions of both experiments into account, the agreement between Sosnowski's results and ours is quite good. The lower slope of the Sosnowski curve can be explained by the wider diameter of his discharge tube, lowering the cataphoresis efficiency.

At higher Cd source temperatures both parts of the Cd atom density distribution, exhibiting a linear and quasiexponential character, respectively, exist (Fig. 12). The slope of the linear part of the distribution curve decreases with decreasing discharge current. At discharge currents lower than 50 mA the gradient of the Cd atom density is so low that the linear part of the distribution reaches the anode region and the discharge becomes unstable. At higher discharge currents both parts of the distribution are so steep that essentially all of the Cd vapor is confined to the PC region adjacent to the Cd source. The shapes of the quasiexponential parts of the Cd atom density distributions are the same as those obtained for the lower Cd source

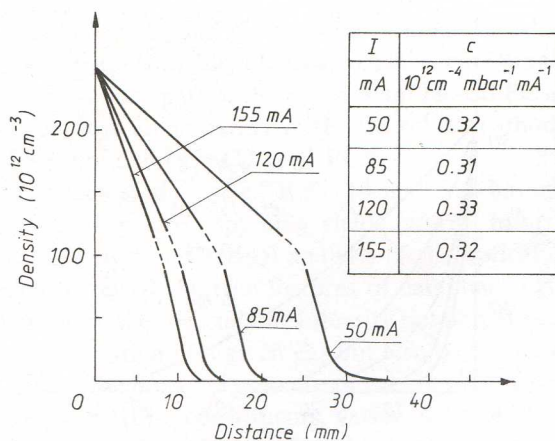


FIG. 12. Axial Cd atom density distributions between the Cd source (at 0 mm) and the anode in the He-Cd PC at a relatively high temperature of the Cd source (550.5 K) for various discharge currents, at  $p=4$  mbar. The table shows the values of the parameter  $c$  appearing in Eq. (1).

temperature (Fig. 11), but due to the higher Cd source temperature the quasiexponential distribution curves are displaced towards the anode. The displacement is larger for lower discharge currents.

Figure 13 shows the He pressure dependence of Cd atom density distribution at constant Cd source temperature and discharge current. The slopes of both parts of the distribution, having a linear and quasiexponential character, respectively, steepen with increasing He pressure. As a result, at higher He pressures the Cd atom density distributions are confined to the PC region near the Cd source.

Simultaneous presence of the two parts (linear and exponential) of the admixture atom density distribution in a glow discharge in a binary mixture was predicted by Druyvesteyn.<sup>39</sup> According to Druyvesteyn's theory the admixture atom density decreases linearly from the cathode

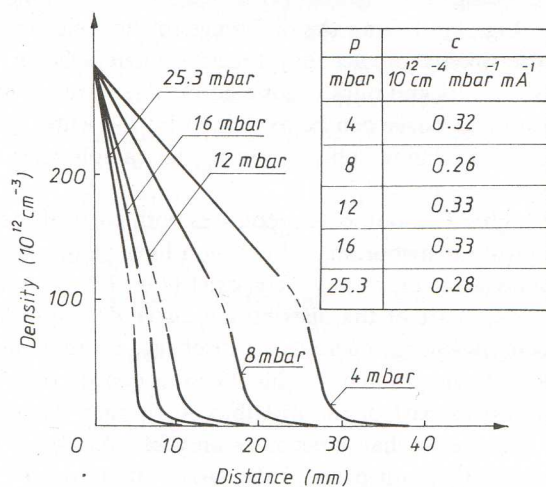


FIG. 13. Axial Cd atom density distributions between the Cd source (at 0 mm) and the anode in the He-Cd PC at a relatively high Cd source temperature (550.5 K) for various He pressures, at  $I=50$  mA. The table shows the values of the parameter  $c$  appearing in Eq. (1).

toward the anode provided that the admixture atom density is sufficiently high. After reaching a certain relatively low value the admixture atom density starts to decrease exponentially. Experimental confirmations of the simultaneous presence of two parts of the admixture atom density distribution are rather scarce (Krysmanski<sup>9</sup> for He-Kr, Schmeltekopf<sup>14</sup> for He-Kr, and Riesz and Diecke<sup>33</sup> for He-Ne and Ne-Ar mixtures). Linear or exponential decays of the axial distribution of the admixture atom density were observed separately for abundant or poor filling of the discharge with the admixture gas by Freudenthal<sup>16</sup> in Ne-Ar and Sanctorum<sup>40</sup> in Ne-N<sub>2</sub> mixtures. One may find other evidence of the simultaneous existence of the two parts of the admixture atom density distribution in the papers of Tombers and co-workers (in He-N<sub>2</sub>),<sup>10</sup> Tombers and Chanin (in Ne-Hg),<sup>11</sup> Hackam (in Ne-Ar),<sup>12</sup> Gaur and Chanin [in He-Ne,<sup>18</sup> He-Ar (Ref. 22)], Hackam,<sup>20</sup> and Hackam and Vincent<sup>23</sup> (both in He-Ar). In this paper the simultaneous presence of the linear and quasiexponential parts of the Cd atom density distribution in the He-Cd PC is demonstrated rather clearly.

After Druyvesteyn<sup>39</sup> the discharge current and He pressure dependence of the linear part of the axial distribution of the Cd atom density  $N$  along the He-Cd PC may be expressed as

$$N(x) = N(x=0) - cpIx, \quad (1)$$

where  $x$  is the distance from the Cd source, and  $c$  is parameter assumed to be constant. If Eq. (1) holds in the case of a He-Cd mixture, the parameter  $c$  should be independent of both discharge current and He pressure. Indeed the values of the parameter  $c$  determined for various discharge currents and He pressures from the linear parts of the distributions presented in Figs. 12 and 13 are close to each other (see the tables inserted in Figs. 12 and 13). Therefore, in the limit of experimental error, it seems that Eq. (1) can be used for describing the linear part of the Cd atom density distribution between the Cd source and the anode in a He-Cd PC, provided that the Cd atom density is higher than about  $100 \times 10^{12} \text{ cm}^{-3}$ . The Druyvesteyn theory, confirmed for the He-Cd mixture in this work, was earlier experimentally found to hold for He-Kr,<sup>9</sup> He-Ne (pressure dependence only),<sup>14</sup> Ne-Ar,<sup>16</sup> and Ne-N<sub>2</sub> mixtures.<sup>40</sup> In our opinion, apparent agreements with Druyvesteyn's theory claimed in some other works should be taken cautiously due to misinterpretation of the linear and exponential parts of admixture atom density distributions. The disagreements of the experimental results with Druyvesteyn's theory noticed by other authors are most likely caused by variations of the discharge conditions during the run of the experiments (e.g., variation of the gas temperature with increasing discharge current<sup>14</sup>).

Druyvesteyn<sup>39</sup> also developed a theory of the exponentially decreasing part of the admixture atom density in the PC in a binary mixture of gases. Although the Cd atom density distributions measured by us exhibit a quasiexponential character, a comparison with Druyvesteyn's theory might be misleading at this stage. This stems from the ambiguity of the estimation of the Cd atom density in the



very tail of its axial distribution. The nonzero intensities of the atomic (and ionic) Cd lines in the distribution tails (Fig. 10) may be evidence of the presence of Cd vapor in the heliumlike part of the PC. On the other hand, a supplementary experiment showed that the measured nonzero intensity distribution tails of the atomic and ionic Cd lines can be due to background scattering (by the discharge tube, oven parts, and deposits on the inner wall of the PC capillary) of the light emitted in all directions by the luminous, cadmiumlike discharge part of the PC. This leads us to believe that the intensity distribution in the very end of the tails are due to the background only. This would mean that part of the He-Cd PC nearest to the anode is free from Cd vapor. If so, the confinement of cadmium vapor due to cataphoresis would be perfect. It is noteworthy that similar difficulties in interpreting the origin of the unexpectedly long axial distribution tails in different mixtures were met by other investigators [Krysmanski in He-Kr,<sup>9</sup> Tombers and co-workers in He-Ne,<sup>10</sup> Tombers and Chanin in Ne-Hg and Ne-Xe-Hg,<sup>11</sup> Hackam in Ne-Ar (Ref. 12) and He-Ar,<sup>20</sup> and Hackam and Vincent in He-Ar mixtures<sup>23</sup>].

#### IV. SUMMARY AND FINAL CONCLUSIONS

Measurements of the axial distributions of the Cd 479.9 nm, Cd<sup>+</sup> 441.6 nm, and He 447.2 nm line intensities as a result of cataphoresis in a He-Cd capillary PC between a Cd source, placed at the cathode side, and an anode were carried out using the method of optical scanning along the PC. The procedure presented in Sec. III allowed us to determine the Cd atom density distributions along the PC.

In this experiment, which was performed differently than most previous studies on cataphoresis, the admixture atom density at the cathode side of the PC could be controlled by varying the Cd source temperature or keeping it constant while changing the discharge current and main gas pressure. This freedom of regulating the Cd atom density at the cathode side of the PC allowed determination of the axial distribution of the Cd atom density.

The nature of the three regions of the He-Cd PC (the cadmiumlike discharge region, the transition region, and the heliumlike discharge region) observed with the naked eye was disclosed to some extent by optical scanning measurements and by the interpretation procedure. We find that in the seemingly uniform, blue-colored cadmiumlike discharge region of the PC, the Cd atom density decreases linearly from the Cd source toward the anode. After reaching a value of  $100 \times 10^{12} \text{ cm}^{-3}$  the Cd atom density decrease changes from linear to quasiexponential, and the so-called transition region, whitish in color, begins. However, the measurements do not answer the question whether Cd atoms are present in the orange, heliumlike discharge region of the PC. Although in this experiment we could not prove that the tail of the Cd atom density distribution ceases in the heliumlike discharge part of the PC, the relatively strong background scattering of the light emitted by the cadmiumlike discharge part of the PC makes us inclined to believe that this region is indeed free

from Cd vapor. Thus the ambiguity and controversy on the cataphoretic confinement in the He-Cd PC remains.

It is shown that the linear and quasiexponential parts of the Cd atom density distribution are present simultaneously in the He-Cd PC if the Cd atom density in the Cd source is higher than about  $100 \times 10^{12} \text{ cm}^{-3}$ . With increasing Cd atom density in the Cd source the linear part extends further, shifting the quasiexponential part toward the anode. At sufficiently high Cd atom density the linear part reaches the anode region of the discharge tube and the discharge becomes unstable. At Cd atom densities in the source lower than about  $100 \times 10^{12} \text{ cm}^{-3}$  only the quasiexponential part exists. Decreasing the Cd atom density in the source shortens the quasiexponential Cd atom density distribution, but it does not change the distribution shape. Comparison of these results with those previously obtained by others indicates that the simultaneous presence of the linear and exponential parts of the admixture atom density distribution is characteristic of a binary gas mixture PC. In our opinion this effect of cataphoresis has been overlooked in some previous investigations.

The slope of the Cd atom density distribution curve in its linear part is found to be proportional to the product of the discharge current and He pressure. This is in good agreement with Druyvesteyn's prediction.<sup>39</sup> The slope of the quasiexponential part of the Cd atom density distribution curve first increases, then saturates, with increasing discharge current and He pressure.

The so-called quality of cataphoresis, defined as the distance from the anode to a point where a marked change in the distribution of the admixture line intensity or the admixture atom density along the PC occurs, is determined by the length of the linear part of the distribution. Therefore, this experiment demonstrates that the quality of cataphoresis in the He-Cd PC decreases with increasing Cd atom density in the source, and increases with increasing discharge current and He pressure. This means that at low Cd atom density and high discharge current and He pressure, most of the Cd vapor in the PC is confined to the region adjacent to the Cd source. We find that for a He-Cd mixture the distance between the Cd<sup>+</sup> 441.6 nm line intensity maximum and the anode region is a convenient and more precise measure of the quality of cataphoresis.

Although the ability of cataphoresis to confine the Cd vapor at the cathode side of the PC could not be determined in this experiment, it does allow the following practical advice for best design of the cataphoretic confinement of the PC and HCD ion He-metal-vapor lasers to be given: The cataphoretic confinement, even if not perfect, can be very effective unless the length of the confinement section is shorter than the total length of the linear and quasiexponential parts of the admixture atom density distribution along a given PC. For the PC ion He-metal laser, the confinement section length can be shorter than for the HCD ones. This follows since the metal-vapor density in the PC lasers is relatively low and, hence, the metal atom density distribution in the PC exhibits only quasiexponential decay, whereas in the HCD, operating at higher metal-vapor density, both parts of the distribution, linear and quasiex-

ponential, appear. On the other hand, the HCD lasers operate at higher discharge currents and He pressures, which make both parts of the distribution shorter. Figures 11–13 can be helpful in estimating the confinement section length over a wide range of discharge parameters, if the diameter of the capillary PC is 3 mm. For capillary PC's of diameters wider or narrower than 3 mm one can expect the confinement section lengths to be longer or shorter, respectively, than for the 3 mm capillary PC.<sup>9,13,14,17,41</sup>

Although this study concerns He-Cd mixtures, the results obtained can be at least informative for cataphoresis in capillary PC's in other He-metal-vapor mixtures used in lasers as well as in nonlasing mixtures, provided the difference between the ionization potentials of the mixture constituents is similar to that of helium and cadmium.

#### ACKNOWLEDGMENT

The authors are grateful to Mr. Levi Claesson for skilful manufacture of the discharge tubes.

#### APPENDIX: INTENSITY OF THE Cd 479.9 nm LINE AS A FUNCTION OF Cd ATOM DENSITY

The relation between the sidelight intensity of the Cd 479.9 nm line and the density of Cd atoms in the He-Cd PC, needed for the calibration procedure described in Sec. III, can be determined using a cataphoretic He-Cd laser discharge tube.<sup>4-6</sup> In such a tube the cataphoretic transport of Cd<sup>+</sup> ions from the Cd source toward the cathode produces an axially uniform He-Cd PC between the Cd source and the cathode, with a constant axial distribution of the Cd atom density.<sup>6,35</sup> Knowing the Cd source temperature, the Cd atom density dependence of the Cd 479.9 nm line intensity can be determined. Alternatively, a more reliable but more complicated absorption method<sup>38</sup> can be employed. The accuracy of the former method, used in this experiment, depends strongly on the influence of the discharge conditions on the Cd atom density in the Cd source. The less the Cd atom density in the Cd source depends on the discharge conditions, the higher is the accuracy of determining the Cd density in the He-Cd PC. Usually a Cd sidearm reservoir having an outlet to the PC capillary as large as possible and being thermally isolated from the discharge tube meets the above requirement for high measurement accuracy.<sup>35</sup>

The discharge tube used in the measurement of the Cd 479.9 nm line intensity as a function of the Cd atom density in the He-Cd PC was a typical He-Cd PC laser tube. The PC section of the tube was a Pyrex capillary having an inner diameter of 3 mm and a length of 25 cm. A sidearm-type Cd reservoir, thermally isolated from the discharge tube, was attached to the capillary 5 cm from the anode end of the capillary. The outlet from the Cd reservoir to the capillary was as large as technically possible. The other arrangements—the four separate ovens for the cathode, Cd source, capillary PC, and anode regions, the gas reservoir of a large volume, etc., as well as the operating and measuring procedures—were similar to those used in the principal experiment. The sidelight intensities of the Cd 479.9

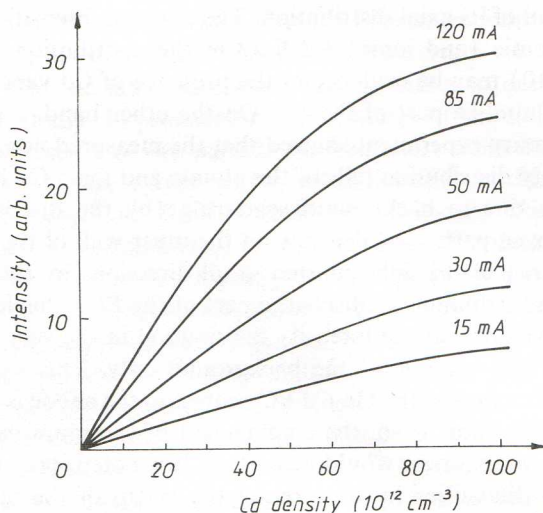


FIG. 14. Intensity of the Cd 479.9 nm line as a function of Cd atom density in the He-Cd PC of 3 mm diameter for various discharge currents at  $p=4$  mbar.

nm line and other relevant Cd, Cd<sup>+</sup>, and He lines were measured in the center of the capillary PC, 10 cm from the Cd source. The temperature of the Cd source was measured using a thermocouple. The Cd saturated vapor pressure in the Cd source was found from the diagram given by Roth.<sup>21</sup> The Cd atom density in the Cd source, assumed equal to the Cd atom density in the He-Cd PC, was calculated from the equation of state of an ideal gas.

An example of the dependence of the sidelight intensity of the Cd 479.9 nm line on the Cd atom density is presented in Fig. 14. It shows that the Cd 479.9 nm line intensity in the He-Cd PC is proportional to the Cd atom density up to at least  $15 \times 10^{12} \text{ cm}^{-3}$ . At higher Cd atom densities the Cd 479.9 nm line intensity exhibits saturation. The Cd 479.9 nm line intensity versus Cd atom density characteristic, shown in Fig. 14 and other similar plots obtained for various discharge conditions, were used as the calibration curves in Sec. III.

The measurements could only be carried out in the Cd atom density range up to  $100 \times 10^{12} \text{ cm}^{-3}$ . This was due to the ionization "waves" which appeared when the Cd atom density was above  $100 \times 10^{12} \text{ cm}^{-3}$ , making the discharge unstable.

In this measurement we also found that the Cd<sup>+</sup> 441.6 nm line intensity reaches its maximum at the Cd atom density  $15 \times 10^{12} \text{ cm}^{-3}$ , and that the Cd 479.9 nm line intensity levels off at about  $100 \times 10^{12} \text{ cm}^{-3}$ . This is in good agreement with the results of Mori *et al.*,<sup>27,36,37</sup> Mizieraczyk,<sup>35</sup> and Goto and co-workers.<sup>38</sup>

<sup>1</sup>L. Laška, Česk. Čas. Fiz. Sekce A 22, 484 (1972).

<sup>2</sup>L. M. Chanin, in *Electrical Discharge*, edited by M. N. Hirsch and H. J. Oskam (Academic, New York, 1978), pp. 133–171.

<sup>3</sup>C. S. Willet, *Introduction to Gas Lasers: Population Inversion Mechanisms* (Pergamon, New York, 1974), pp. 191–239.

<sup>4</sup>J. P. Goldsborough, Appl. Phys. Lett. 15, 159 (1969).

<sup>5</sup>J. R. Fendley, Jr., I. Gorog, K. G. Hernquist, and C. Sun, RCA Rev. 30, 422 (1969).

<sup>6</sup>T. P. Sosnowski, J. Appl. Phys. 40, 5138 (1969).

- <sup>7</sup>K. G. Hernquist, *Appl. Phys. Lett.* **16**, 464 (1970).
- <sup>8</sup>K. G. Hernquist, *IEEE J. Quantum Electron.* **QE-8**, 740 (1972).
- <sup>9</sup>K. H. Krysmanski, *Ann. Phys. (Leipzig)* **7**, 263 (1958).
- <sup>10</sup>R. B. Tombers, J. P. Gaur, and L. M. Chanin, *J. Appl. Phys.* **42**, 4855 (1971).
- <sup>11</sup>R. B. Tombers and L. M. Chanin, *J. Appl. Phys.* **44**, 3087 (1973).
- <sup>12</sup>R. Hackam, *J. Appl. Phys.* **45**, 2880 (1974).
- <sup>13</sup>H. D. Beckey, W. E. Groth, and K. H. Welge, *Z. Naturforsch. A* **8**, 556 (1953).
- <sup>14</sup>A. L. Schmeltekopf, Jr., *J. Appl. Phys.* **35**, 1712 (1964).
- <sup>15</sup>J. Freudenthal, *Physica* **36**, 354 (1967).
- <sup>16</sup>J. Freudenthal, *Physica* **36**, 365 (1967).
- <sup>17</sup>F. H. Shair and D. S. Remer, *J. Appl. Phys.* **39**, 5762 (1968).
- <sup>18</sup>J. P. Gaur and L. M. Chanin, *J. Appl. Phys.* **40**, 256 (1969).
- <sup>19</sup>R. B. Tombers and L. M. Chanin, *J. Appl. Phys.* **41**, 2433 (1970).
- <sup>20</sup>R. Hackam, *J. Appl. Phys.* **44**, 3113 (1973).
- <sup>21</sup>A. Roth, *Vacuum Technology* (North-Holland, Amsterdam, 1976), pp. 147-161.
- <sup>22</sup>J. P. Gaur and L. M. Chanin, *J. Appl. Phys.* **41**, 106 (1970).
- <sup>23</sup>R. Hackam and P. L. Vincent, 2nd International Conference on Gas Discharges Institution of Electrical Engineers, Savoy Place, London, 11-15 September 1972, pp. 65-67.
- <sup>24</sup>W. Muller and E. F. Tubbs, *J. Appl. Phys.* **34**, 969 (1963).
- <sup>25</sup>J. Mizeraczyk, *Bull. Acad. Pol. Sci. Ser. Sci. Tech.* **23**, 43 (1975).
- <sup>26</sup>W. T. Silfvast, *Phys. Rev. Lett.* **27**, 1489 (1971).
- <sup>27</sup>M. Mori, M. Murayama, T. Goto, and S. Hattori, *IEEE J. Quantum Electron.* **QE-14**, 477 (1978).
- <sup>28</sup>G. M. Malyshev and B. W. Pavlov, *Vestn. Leningrad. Univ.* **16**, 34 (1957).
- <sup>29</sup>H. Morgenroth, *Ann. Phys. (Leipzig)* **7**, 373 (1959).
- <sup>30</sup>R. H. Springer and B. T. Barnes, *J. Appl. Phys.* **39**, 3100 (1968).
- <sup>31</sup>D. A. Lee and A. Garscadden, *Phys. Fluids* **15**, 1826 (1972).
- <sup>32</sup>T. F. Johnson, Jr. and W. P. Kolb, *IEEE J. Quantum Electron.* **QE-12**, 482 (1976).
- <sup>33</sup>R. Riesz and G. H. Diecke, *J. Appl. Phys.* **25**, 196 (1954).
- <sup>34</sup>S. E. Frish and N. A. Matveeva, *Dokl. Akad. Nauk SSSR* **122**, 375 (1958).
- <sup>35</sup>J. Mizeraczyk, Ph.D. thesis, University of Gdańsk, Gdańsk, Poland, 1975.
- <sup>36</sup>M. Mori, K. Takasu, T. Goto, and S. Hattori, *J. Appl. Phys.* **48**, 2226 (1977).
- <sup>37</sup>M. Mori, T. Goto, and S. Hattori, *J. Phys. Soc. Jpn.* **44**, 1715 (1978).
- <sup>38</sup>T. Goto, M. Mori, and S. Hattori, *Appl. Phys. Lett.* **29**, 358 (1976).
- <sup>39</sup>M. J. Druyvesteyn, *Physica* **2**, 255 (1935).
- <sup>40</sup>C. Sanctorem, in *Proceedings of the Twelfth International Conference of Phenomena in Ionized Gases*, Eindhoven, Netherlands, edited by J. G. A. Hölscher and D. C. Schram (North-Holland/American Elsevier, Amsterdam, 1975), p. 70.
- <sup>41</sup>J. Freudenthal, *J. Appl. Phys.* **38**, 4818 (1967).